

Micro-CT study of the Impact of Low Salinity Waterflooding on the pore-scale fluid distribution during flow

W.-B. Bartels^{1,2}, M. Rücker^{1,3}, S. Berg¹, H. Mahani¹, A. Georgiadis^{1,8}, N. Brussee¹, A. Coorn¹, H. van der Linde¹, A. Fadili¹, C. Hinz⁴, A. Jacob⁴, C. Wagner⁵, S. Henkel⁶, F. Enzmann⁴, A. Bonnin⁷, M. Stampanoni⁷, H. Ott^{3,9}, M. Blunt³, S.M. Hassanizadeh²

¹ Shell Global Solutions International B.V., Kesslerpark 1, 2288 GS Rijswijk, The Netherlands

²Earth Sciences department, Utrecht University, 3584 CD Utrecht, The Netherlands

³ Department of Earth Science and Engineering, Imperial College London, SW7 2AZ UK

⁴Geosciences Institute, Johannes Gutenberg-University, Becherweg 21, 55099 Mainz, Germany

⁵ Math2Market GmbH, Stiftsplatz 5, 67655 Kaiserslautern, Germany

⁶ Institute of Geosciences, Friedrich Schiller University Jena, Burgweg 11, 07743 Jena, Germany

⁷ Swiss Light Source, Paul Scherrer Institute, CH-5232 Villigen, Switzerland

⁸ Department of Chemical Engineering, Imperial College London, SW7 2AZ UK

⁹ Department of Petroleum Engineering, Montanuniversität Leoben, A-8700 Leoben, Austria

This paper was prepared for presentation at the International Symposium of the Society of Core Analysts held in Snowmass, Colorado, USA, 21-26 August 2016.

ABSTRACT

Many studies indicate that the recovery of crude oil by waterflooding can be improved in both sandstone and carbonate rocks by lowering the salinity of injected water. This so-called low salinity effect is thought to be associated with the change of the wetting state of rock towards more water wet. However, it is not very well understood how wettability alteration on the pore level could lead to an increase in production at the Darcy scale. Therefore, this study aims at direct pore scale observation of the wettability-change-driven fluid reconfiguration related to a low salinity (LS) flood at the length scale between a single pore and the Darcy scale (i.e. pore network scale). We investigate the low salinity effect in real time and in 3D using synchrotron beamline-based fast X-ray computed tomography during flow experiments.

Cylindrical outcrop rock samples of 20 mm length and 4 mm diameter were initialized by first saturating them with high salinity (HS) brine and then with crude oil. Subsequently, they were aged at 30 bars and 70°C for one week in order to establish wettability states assumed close to reservoir conditions. The synchrotron beamline-based fast tomography allowed us to image the pore scale fluid distribution at a spatial resolution of 3 μm and (under flowing conditions) at time intervals of 10 s for a full 3D image.

The micro-CT flow experiments were conducted on both sandstone and carbonate rocks, all in tertiary mode, i.e. by first performing a HS water flood i.e. forced imbibition (as base-line) followed by a LS waterflood, both at identical field relevant flow rates. The real-time imaging shows a saturation change during the HS waterflood which approaches a stable equilibrium at its end. When switching to low salinity water, we observe a

change in average saturation and pore scale distribution of both fluids, which is distinctly different from the stabilizing saturation during HS flooding. Compared to the end of the HS flood, during the LS flood in both sandstone and carbonate rock, the oil moves from pore throats to the center of pore bodies. This movement is indicative of a pore scale wettability transition from a mixed wet to a more water wet state. This process involves (re)connection and disconnection of the oil phase as it moves through narrow pore throats which is characteristic of ganglion dynamics.

INTRODUCTION

Low salinity waterflooding (LSF) is an enhanced oil recovery/improved oil recovery (EOR/IOR) technique which mobilizes more oil by modifying and/or lowering the ionic composition of the injected brine. For sandstones, the range at which additional production occurs lies between 1500 and 5000 ppm. Lower salinities may lead to formation damage due to fines migration and plugging. For carbonates, the LS threshold at which the low salinity effect (LSE) occurs lies much higher. There are even cases reported for sea water; see [1] and references therein for a short overview. In addition, the exact brine chemistry is deemed more important for carbonates than for sandstones. The LSE is often described phenomenologically by wettability alteration to a more water-wet state. However, the mechanisms behind the alteration are not fully understood.

Several mechanisms have been proposed in the literature; however, there is no general consensus on the dominant mechanism or mechanisms; see e.g. [2-5]. Moreover, the evidence supporting a particular mechanism is often indirect or inferred from the experimental measurements; and in some cases the evidence is even contradictory. If we examine the body of literature, in general it can be divided into two groups. On the one hand there are studies looking at contact angle changes and detachment of crude oil from mineral surfaces i.e. at sub pore scale. On the other hand there are experiments which look for incremental production of crude oil in core flooding experiments. However, it is not clear how a contact angle change on the sub pore scale leads to additional Darcy scale oil production. There is a gap between the (sub) pore scale and the Darcy scale in which hardly any research has been conducted. Incremental oil production on the Darcy scale requires a change in configuration of oil on the scale of multiple pores, i.e. the pore network scale. The details of this change of oil saturation distribution on the pore network scale is expected to close the gap between surface science and reservoir engineering concepts and provide the links between proposed mechanisms and Darcy scale observation.

In order to investigate the effect of LSF on the configuration of oil on this intermediate pore network scale under flowing conditions, we use synchrotron based fast X-ray tomography.

MATERIALS AND METHODS

Rock samples and brines

For the experiments in this study, we used Berea sandstone [6] combined with reservoir dead crude "S" (density $\rho = 0.87 \text{ g/cm}^3$, viscosity $\eta = 7.87 \text{ mPa}\cdot\text{s}$, at $T = 20^\circ\text{C}$) and

Ketton as carbonate rock with reservoir dead crude “C” ($\rho = 0.83 \text{ g/cm}^3$, $\eta = 4.30 \text{ mPa}\cdot\text{s}$, at $T = 20^\circ\text{C}$). The samples were 20 mm long and 4 mm in diameter and embedded in heat-shrunk PEEK (Polyether Ether Ketone) tubes. As HS brine, we used 200 g/L KI (potassium iodide, ionic strength 0.602 mol/L) and as LS water, 27 g/L KI (ionic strength 0.081 mol/L).

Experimental workflow

A rock sample was first cleaned using isopropanol and then shrunk in PEEK. When handling the core, nitrile gloves were used at all times to prevent altering the wettability of the rock upon touch. The sample was then fully saturated with HS brine under vacuum. Subsequently, it was mounted on the flow cell as used in [7, 8] to establish initial water and oil saturation in the sample. When the sample was saturated with HS brine and crude oil, the initial wettability state was established by aging it submerged in crude oil at 30 bars and 70°C for one week. The experimental set-up we used has been described in [7, 8], where the two cylinders of the in-situ pump were used for fractional flow experiments. In this study, the cylinders were filled with HS brine and LS water, respectively, to conduct tertiary LS flooding experiments.

The flooding and X-ray saturation monitoring experiments were performed at the TOMCAT beamline of the Swiss Light Source (Paul Scherrer Institute) which is a fast synchrotron-based X-ray computed micro-tomography facility. In this study, a “pink beam” configuration with a finite X-ray energy spectrum was used. This setting caused significant beam hardening. The flow rate in both high and low salinity experiments was $30 \mu\text{l}/\text{min}$ (equivalent to $\sim 12 \text{ ft}/\text{day}$) and injection always occurred from bottom to top. The field of view (FOV) was chosen 2 mm above the inlet, and dimensions of the monitored area were approximately 4 mm laterally and 3 mm along the principal axis of the sample. A full 3D image with a voxel size of $3 \mu\text{m}$ was obtained within about 7 s. The transition from HS flooding to LS flooding was monitored continuously for 5 min. In addition, images from 30 minutes before to 30 minutes after the transition were recorded at a rate of 1 image/min.

Image processing

The images were reconstructed using the Paganin method [9, 10] since the end result was found superior to that of the attenuation contrast reconstruction method, as shown in **Figure 1**. The reconstructed micro-CT images were filtered, segmented, and processed with the software package AVIZO 9.0 and 8.1 (FEI). A combination of gradient images and watershed segmentation led to satisfactory results. After segmentation, the binarized images are analyzed further.

RESULTS AND DISCUSSION

Potential Imaging Artifacts

The processed grey scale images before segmentation, such as the one for the oolitic carbonate rock shown in **Figure 2**, show a clear contrast difference between grains, the doped brine (at HS), and a dark phase which should contain the oil. However, a more

detailed inspection reveals a grey-scale variation and a structure inside the darkest phase, see

Figure 3, which occurs systematically for all samples studied. That raises the suspicion that a third fluid phase may be present and brings up several questions about

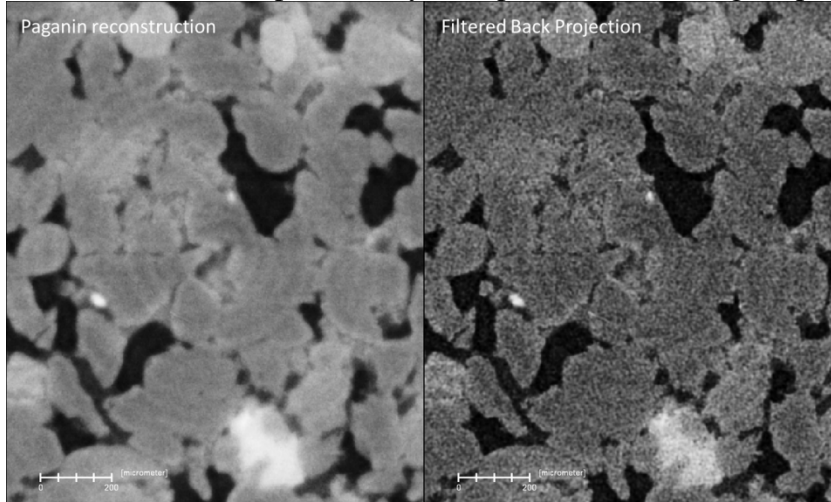


Figure 1: Difference in image quality by reconstructing Berea sandstone with Paganin (left) and Filtered Back Projection (right) algorithms. There is a clear difference in noise level and contrast between the two methods. The scale bar indicates 200 micrometer.

significance and interpretation of the images and the origin of the phases that are visible. This is discussed in the following sections.

Possible explanations for the apparent presence of three phases are:

- A) artefacts related to reconstruction, filtering and beam hardening,
- B) trapping of gas during sample preparation,
- C) gas formation due to X-ray exposure,
- D) degassing of crude oil due to X-ray exposure,
- E) discoloration of a part of the brine phase due to brine-rock interaction such as ion exchange and adsorption
- F) formation of oil/water structures.

Some of these possibilities are more likely than others. The questions that arise are: is this an artifact that invalidates the experiment as such (items B-D) or an artifact that complicates the data analysis (A); are the experiments in principle valid; or are we actually dealing with a relevant phenomenon (E-F).

Note that we have observed these effects in all our synchrotron beamline LSF experiments in both sandstone and carbonate samples. Explanations B, C and D relate to the origin of the darkest phase, suggesting that the intermediate phase is oil and the bright phase is HS brine. Explanations D and E assume that the intermediate phase is the anomalous phase i.e. something other than oil or brine. Below, we provide a detailed assessment of each explanation.

A) Artefacts related to reconstruction, filtering and beam hardening

Our data shows significant beam hardening. To what extent this effect translates into gray scale variations and structures within pores is not clear. In addition, glow from the HS brine phase and from the grains may elevate the gray levels of the darkest phase in the pore space. Still, the darkest phase seems to be much brighter than the exterior, indicating that it cannot be a gas phase.

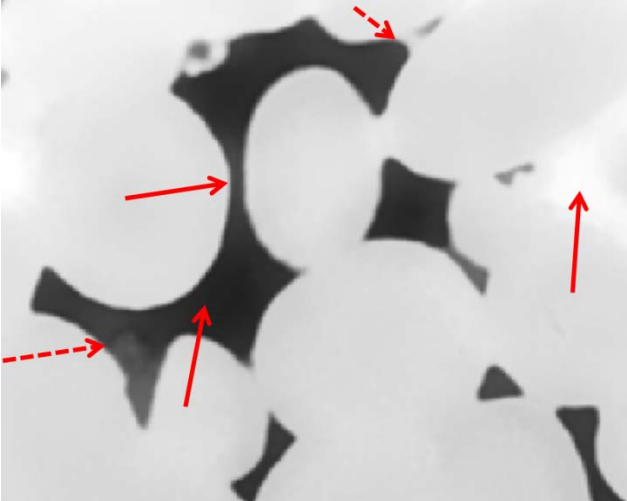


Figure 2: Different gray values in the pore space of oolitic carbonate rock. We distinguish between bright, intermediate and dark phases. In some cases, interfaces are visible, see dashed arrows.

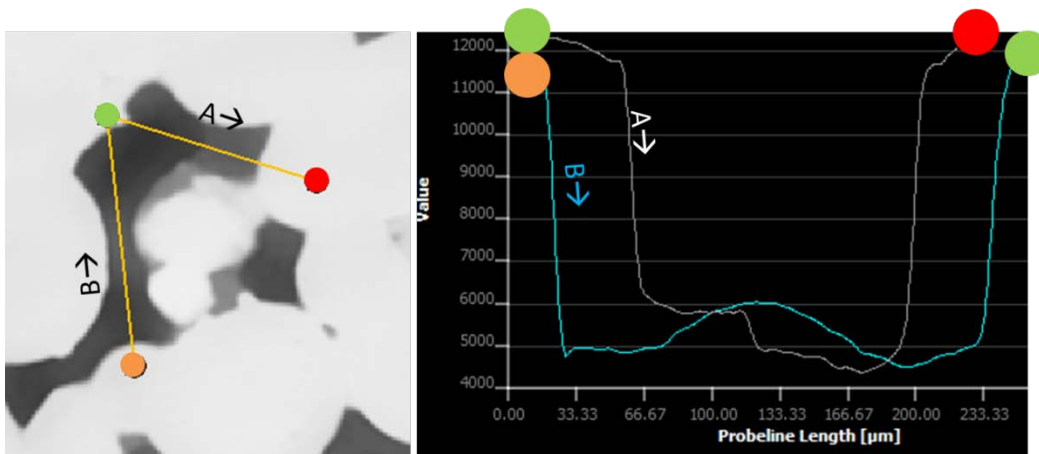


Figure 3: Stepped change in gray value and gradual changes in gray value overlap making segmentation difficult. This example was taken from carbonate rock.

B) Trapping of gas during sample preparation

After the preparation of the samples at Shell laboratories, micro-CT scans with a benchtop instrument (ZEISS Xradia 520 Versa) were made. Benchtop machines use a much broader and higher energy X-ray spectrum but at several orders of magnitude lower intensity. In those scans, no such variation in the darkest phase was observed; at least, the formation of a separate gas phase could be ruled out. After preparation of the samples, in-house micro-CT scans only revealed two sets of gray levels: that of HS brine (bright) and oil. In cases that air and/or gas had been accidentally trapped in the pore space, this was

clearly recognizable in the in-house scans and these samples had been excluded from further analysis. However, imaging at the synchrotron beamline – approximately after one week of aging – revealed the situation shown in **Figure 2** in all samples. So, unless a gas phase forms (C, D) upon exposure to the much higher intensity synchrotron beam, explanation (B) can be ruled out.

C) Gas formation due to X-ray exposure

In previous beamline experiments, the formation of bubbles has been observed, but it was also found that occurrence and magnitude of the effect depended on beam energy, intensity, type of fluid, and dopant concentration. While the reason was ultimately not clear, a photochemical effect was discussed as the most likely cause. In order to assess whether the darkest phase in **Figure 2** could be in-situ formed gas bubbles, we conducted a long-time exposure experiment to see if the specific beam settings used in this study would lead to bubble formation as well. Similarly to previous studies, we observed bubble formation in the (doped) brine phase, as shown in **Figure 4**, but no formation of gas bubbles in the oil phase were observed. Morphology and growth kinetics of the bubbles are very different from the structure in the darkest phase in **Figure 2**. In addition, if the bubbles have a photochemical origin, one would expect the process to occur or intensify when freshly doped HS brine was injected in the system. Examining saturation of the dark, intermediate and bright phase versus time displayed in **Figure 7** does not show such an increase. Therefore, (C) is also very unlikely.

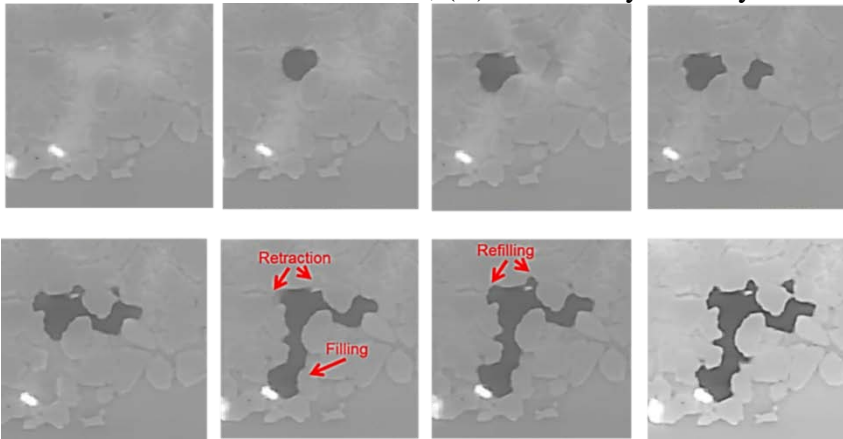


Figure 4: Bubble formation in sandstone only filled with strongly doped HS brine. There was no flow during this experiment. The images are taken with intervals of 10 seconds.

D) Degassing of crude oil

When the temperature is increased or the pressure is decreased, light hydrocarbon components present in the crude oil may come out of solution and form gas bubbles. However, the temperature during transport and experimentation did not increase by more than 2 °C. In addition, the pressure was constant. Given that both crude oils were “dead crude” (i.e. degassed crude) with the bubble point being far away from conditions in the experiment, (D) is very unlikely.

E) Discoloration of part of the brine phase

Some of the intermediate grey levels could represent brine with a reduced concentration of contrast agent KI. One might speculate that such a compositional change might have occurred through brine-rock interactions, such as ion exchange reactions with the solid, or adsorption. However, the laws of thermodynamics would prohibit any spontaneous demixing. Another counter-argument is that when the intermediate grey level is classified as a brine phase, it implies very low initial oil saturation. In addition, if the intermediate grey levels are interpreted as a separate phase, then the observation of a “contact angle” with the brine phase would rule out an aqueous phase even though the phase is mostly located in the corners of pores.

F) Formation of oil/water structures

Oil-brine mixing tests revealed that the crude oils used in this study can form oil/water structures, such as emulsions, when in contact with brine. This is shown in **Figure 5**.

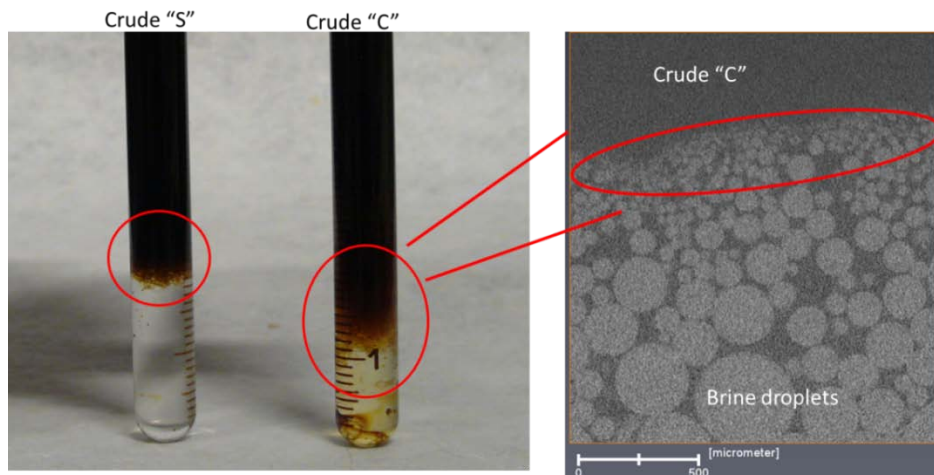


Figure 5: Different degrees of oil/water structure formation for crude “S” and “C”. The right hand side shows a benchtop micro-CT scan of the interface between crude “C” and emulsion. The encircled portion of this image shows droplets below the imaging resolution.

Such structures have also been described by others [11-13]. The gray values of these oil/water structures would lay in between that of the pure phases. Any micro-structure i.e. individual droplets may be significantly blurred given the limited spatial resolution of the micro-CT and imaging artifacts discussed in (A).

In summary, the development or presence of a gas phase (explanations B-D) and the presence of a second brine phase (E) seem unlikely. Certainly, imaging and reconstruction artifacts occur (A) and if these are solely responsible for the variation of grey levels, all should be lumped into the oil phase. But the formation of oil/water structures (F) could occur as observed in tube tests under similar conditions (see **Figure 5**). Because of the potential connection of gray-scale feature to a LSE [12, 13] it might therefore be beneficial to treat it until further clarification as a separate phase.

In the following we will discuss the response to LS and focus in particular on the aspects that are robust against the considerations A-F. Therefore we will focus on the behavior of the darkest phase.

Response to High Salinity

During HS flooding, we see the oil phase clusters disconnecting and reconnecting, which indicates a ganglion dynamics flow regime as observed already in 2D micro-models [14] and other micro-CT imbibition experiments [8], [15], [16]. However, we see oil-filling events covering pore bodies in the mixed-wet condition as shown in **Figure 6**. We did not observe this in previous studies under water-wet conditions.

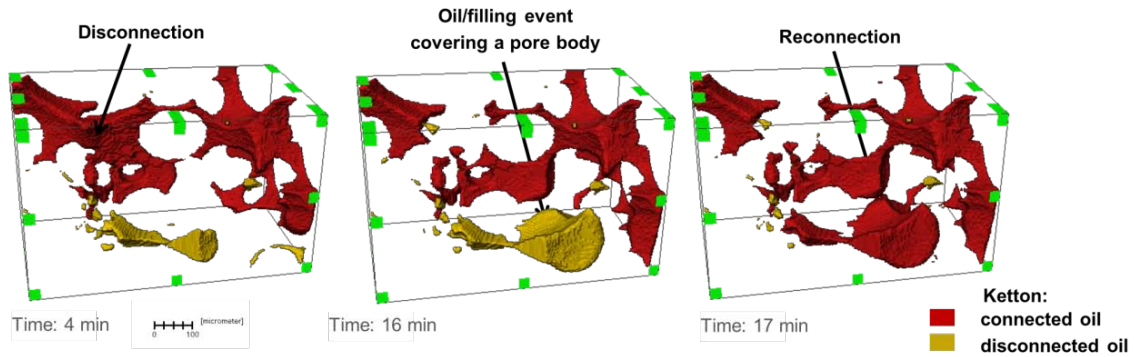


Figure 6: 3D rendering of pore filling event in carbonate (Ketton) rock in HS.

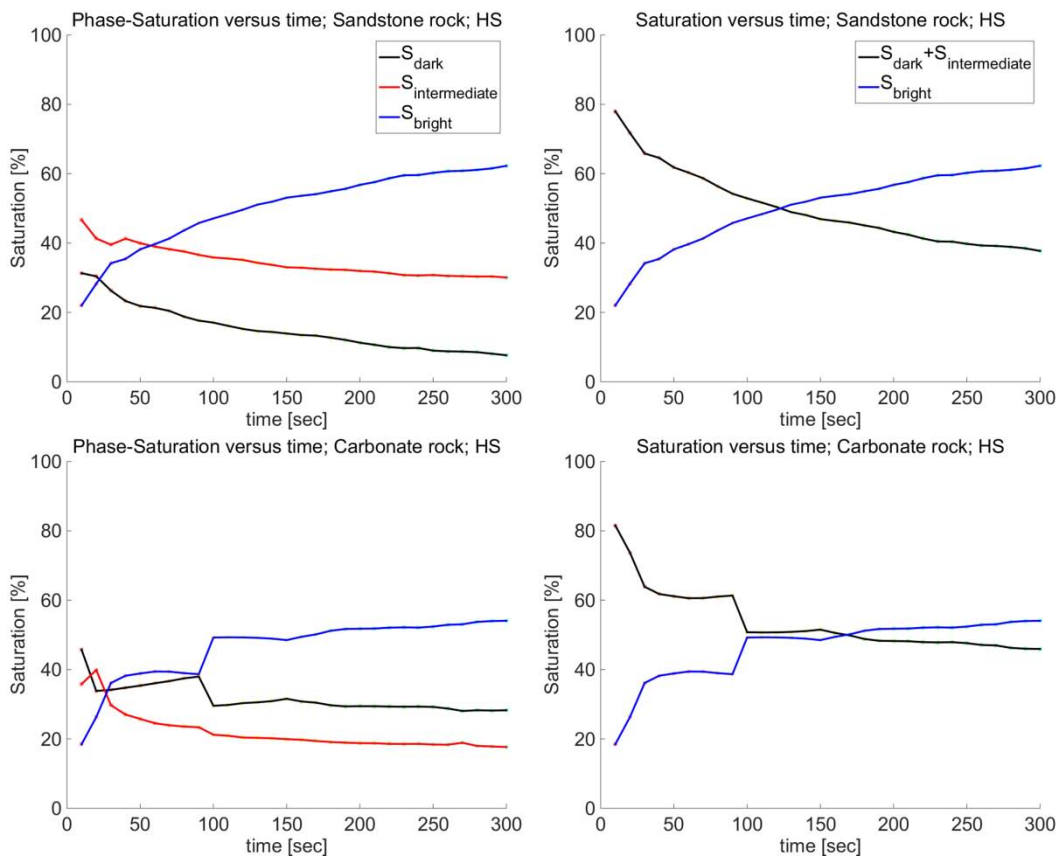


Figure 7: Saturation versus time plots for a HS flood in sandstone and carbonate. The decrease of the darkest phase suggests that it cannot be gas that is created because of X-ray exposure. The initial

saturation suggest that the intermediate gray phase and the dark phase should be considered as the same phase.

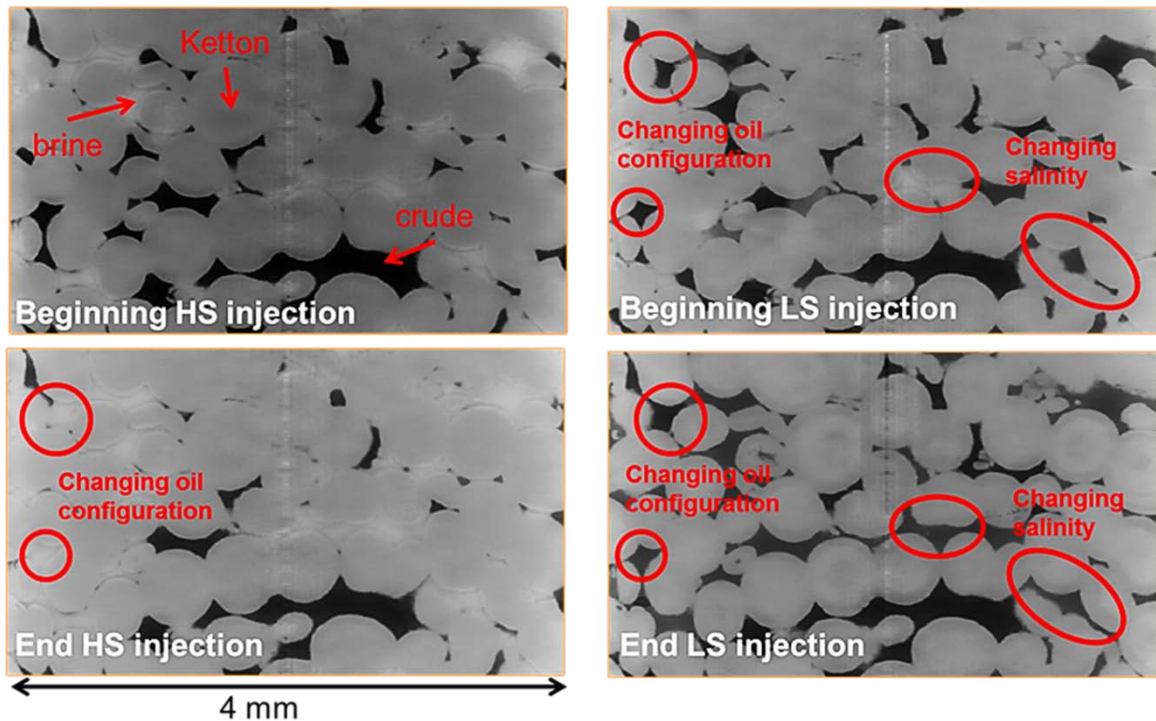


Figure 8: When changing from HS to LS, a clear redistribution of oil can be seen from the pore throats to the pore bodies. This is seen most clearly in Ketton rock (Carbonate).

Response to Low Salinity

The first observation in the images captured during LS is that we can track the change in salinity as the concentration of contrast agent decreases as seen in **Figure 8**. Secondly, we see a change in oil configuration as the oil phase moves from smaller to larger pores at the transition from HS to LS, also shown in **Figure 8**. This is indicative of a wettability alteration towards more water wet, as is expected in a successful LSF experiment. For sandstone, this is intriguing since the salinity level used here is much higher than the generally accepted salinity range of 1500-5000 ppm in which the macroscopic (Darcy) LSE has been typically observed.

Pore filling events

We also observe ganglion dynamics during the LS flood. During LS flooding, we clearly see that the extent of oil displacement is much larger than at the final stages of the HS flood, as illustrated in **Figure 9**. This indicates that the LS water did mobilize more oil, which may have come from the upstream part of the sample outside the FOV. This oil saturation increase in the FOV can be temporary (a transient effect) and could be related to oil banking by LS. The oil bank could eventually be produced from the sample.

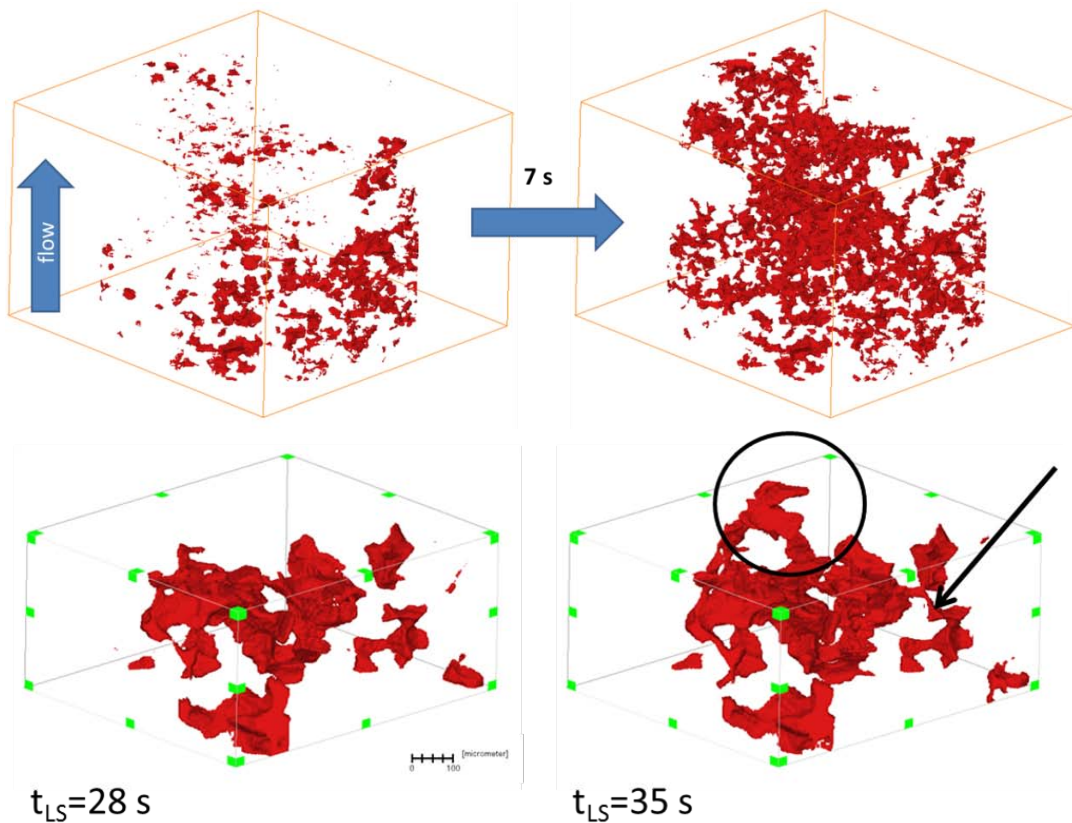


Figure 9: Top: Increase in the darkest phase in 7 seconds in Berea sandstone during LS flooding. This magnitude of increase cannot be caused by gas. In addition, this increase is occurring after the saturation of all phases stabilized during HS flooding, see **Figure 7**. Bottom: Cluster dynamics during LS flow in Berea sandstone. Scale bar indicates 100 micrometer. The circle indicates growth of the oil cluster and the arrow indicates a (re)connection point. Flow is from bottom to top.

CONCLUSIONS

We have observed an additional oil/water structure or a third phase and are not sure of its nature and origin. Further tests need to be conducted to verify whether this oil/water structure is a (micro-) emulsion. Regardless of the occurrence of this structure, we still can draw the following conclusions regarding the LSF experiments.

- We reached a stable saturation during HS flooding.
- During LS injection, we observed the following:
 - i) There is oil redistribution from pore throats to pore bodies, which would correspond to a shift of wettability to a more water wet system.
 - ii) There is an increase in the overall oil saturation in the investigated FOV. This is most likely the mobilized or re-connected oil from upstream and is indicative of a low-salinity effect. The increase of oil saturation can be transient and may be

related to oil banking by LS. The oil bank, because of high saturation and high relative permeability, may eventually be produced from the sample.

Additionally:

- For sandstones, the LSE occurred at relatively high salinities.
- We observed filling events covering multiple pores in both rock types, which we believe to be specific to the mixed wet state of the system.
- We see ganglion dynamics in both HS and LS regimes but in LS we also see remobilization of crude oil.

ACKNOWLEDGEMENTS

We would like to acknowledge the staff of the TOMCAT beamline at the Swiss Light Source of the Paul Scherrer Institute, Villigen, Switzerland for support during the execution of this work. We thank Alex Schwing and Rob Neiteler for the design of the flow set-up and instrumentation, Fons Marcelis for sample preparation, Kamaljit Singh for supplying the Ketton rock and Axel Makurat for helpful discussions and leadership support. We gratefully acknowledge Shell Global Solutions International B.V. for permission to publish this work.

REFERENCES

1. Mahani, H., A. Keya, S. Berg, W.-B. Bartels, R. Nasralla and W. Rossen, "Insights into the Mechanism of Wettability Alteration by Low-Salinity Flooding (LSF) in Carbonates", *Energy and Fuels* (2015), **29**, 1352-1367.
2. Aladasani, A., B. Bai, Y.-S. Wu and S. Salehi, "Studying low-salinity waterflooding recovery effects in sandstone reservoirs", *Journal of Petroleum Science and Engineering* (2014), **120**, 39-51.
3. Morrow, N., and J. Buckley, "Improved Oil Recovery by Low-Salinity Waterflooding", *Journal of Petroleum Technology*, SPE-129421 (2011).
4. Myint, P., and A. Firoozabadi, "Thin liquid films in improved oil recovery from low-salinity brine." *Current Opinion in Colloid & Interface Science* (2015) **20**, 2, 105-114.
5. Lager, A., K. Webb, C. Black, M. Singleton and K. Sorbie, "Low Salinity Oil Recovery – An Experimental Investigation", *Petrophysics* (2008), **49**, 1, 28-35.
6. Berg, S., H. Ott, S.A. Klapp, A. Schwing, R. Neiteler, N. Brussee, A. Makurat, L. Leu, F. Enzmann, J.O. Schwarz, M. Kersten, S. Irvine and M. Stampanoni, "Real-time 3D imaging of Haines jumps in porous media flow", *Proceedings of the National Academy of Sciences* (2013), **110**, 10, 3755-3759.
7. Armstrong, R., H. Ott, A. Georgiadis, M. Rücker, A. Schwing and S. Berg, "Subsecond pore-scale displacement processes and relaxation dynamics in multiphase flow", *Water Resources Research* (2014), **50**, 9162–9176.

8. Rücker, M., S. Berg, R. Armstrong, A. Georgiadis, H. Ott, L. Simon, F. Enzmann, M. Kersten and S. de With, "The fate of oil clusters during fractional flow: trajectories in the saturation-capillary number space", *SCA2015-007*.
9. Paganin, D., S. Mayo, T. Gureyev, P. Miller and S. Wilkins, "Simultaneous phase and amplitude extraction from a single defocused image of a homogeneous object." *Journal of microscopy* (2002) **206**, 1, 33-40.
10. Marone, F., and M. Stampanoni, "Regridding reconstruction algorithm for real-time tomographic imaging." *Journal of synchrotron radiation* (2012), **19**, 1029-1037.
11. Rezaei, N., and A. Firoozabadi, "Macro- and Microscale Waterflooding Performances of Crudes which form w/o Emulsions upon Mixing with Brines", *Energy & Fuels* (2014), **28**, 2092-2103.
12. Sohrabi, M., P. Mahzari, S. Farzaneh, J. Mills, P. Tsois, S. Ireland, "Novel Insights into Mechanisms of Oil Recovery by Low Salinity Water Injection", This paper was prepared for presentation at the SPE Middle East Oil & Gas Show and Conference held in Manama, Bahrain, 8-11 March 2015, *SPE-172778-MS*.
13. Fredriksen, S., A. Rognmo and M. Fernø, "Pore-Scale Mechanisms During Low Salinity Waterflooding: Water Diffusion and Osmosis for Oil Mobilization", paper prepared for presentation at the SPE Bergen One Day Seminar held in Bergen, Norway, 20 April 2016, *SPE-180060-MS*.
14. Avraam, D. and A. Payatakes, "Flow regimes and relative permeabilities during steady-state two-phase flow in porous media", *Journal of Fluid Mechanics* (1995), **293**, 207-236.
15. Berg, S., R. Armstrong, A. Georgiadis, H. Ott, A. Schwing, R. Neiteler, N. Brussee, A. Makurat, M. Rücker, L. Leu, M. Wolf, F. Kahn, F. Enzmann and M. Kersten, "Onset of oil mobilization and non-wetting phase cluster size distribution", *SCA2014-022*, (2014).
16. Youssef, S., E. Rosenberg, H. Deschamps, R. Oughanem, E. Maire, and R. Mokso, "Oil ganglia dynamics in natural porous media during surfactant flooding captured by ultra-fast x-ray microtomography", *SCA2014-023*, (2014).
17. Georgiadis, S. Berg, A. Makurat, G. Maitland and H. Ott, "Pore-Scale micro-CT Imaging: Non-Wetting Phase Cluster Size Distribution During Drainage and Imbibition", *Physical Review E* (2013), **88**, 3.